

Electronic Supplementary Information (ESI) for

Thickness-dependent and anisotropic thermal conductivity of black phosphorus nanosheets

Seong Gi Jeon ^{a,b,†}, Ho Sun Shin ^{a,†}, Yun Hwan Jaung ^{a,c}, Jinho Ahn and Jae Yong Song ^{a,*}

^a Center for Convergence Property Measurement, Korea Research Institute of Standards and Science, Daejeon 34113, Republic of Korea

^b Department of Materials Science and Engineering, Korea Advanced Institute of Science and Technology, Daejeon 34141, Republic of Korea

^c Department of Materials Science and Engineering, Hanyang University, Seoul 04763, Republic of Korea

[†] Equal contributions

* Corresponding author. E-mail addresses: jysong@kriss.re.kr (J.Y. Song)

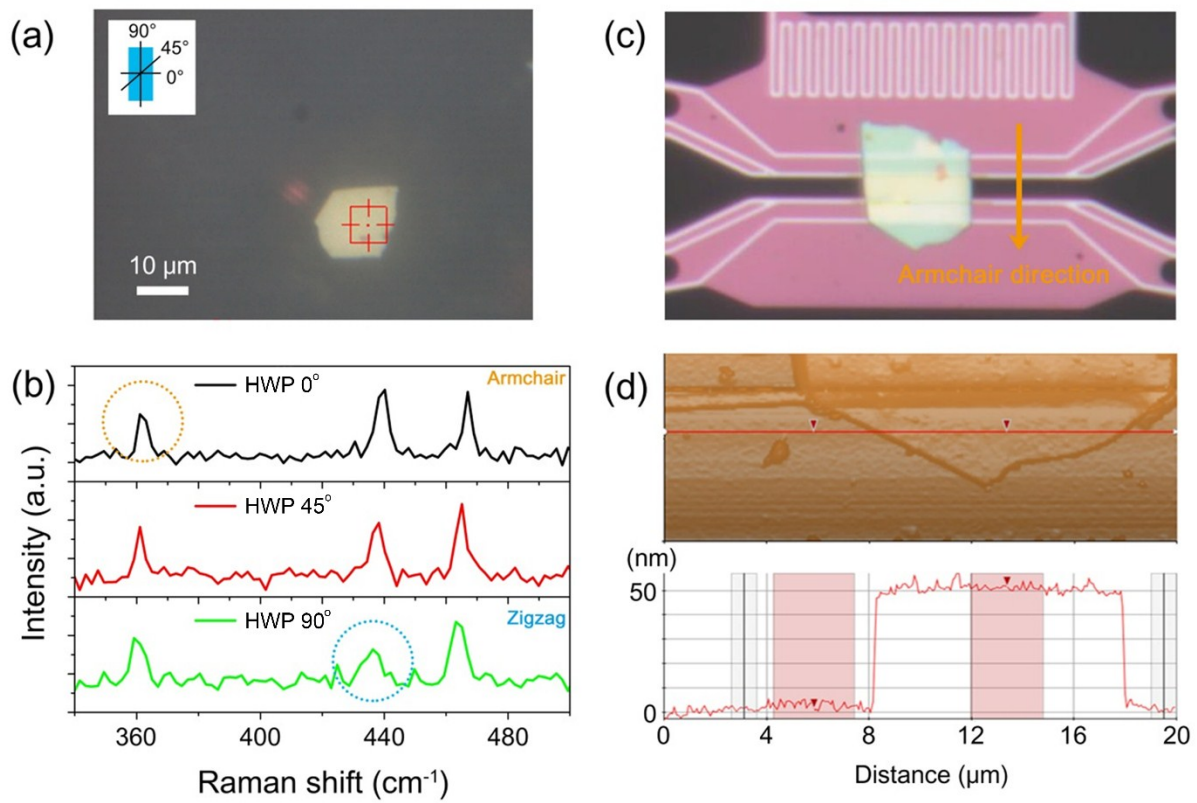


Figure S1. (a) Optical image of a BP NS on AAO template and schematic diagram of the polarization direction of incident laser depending upon the HWP rotation. (b) Raman spectra of a BP NS with the polarization direction of incident laser. (c) Optical image of a BP NS on a microdevice. (d) AFM characterization of the thickness (44 nm) of a BP NS.

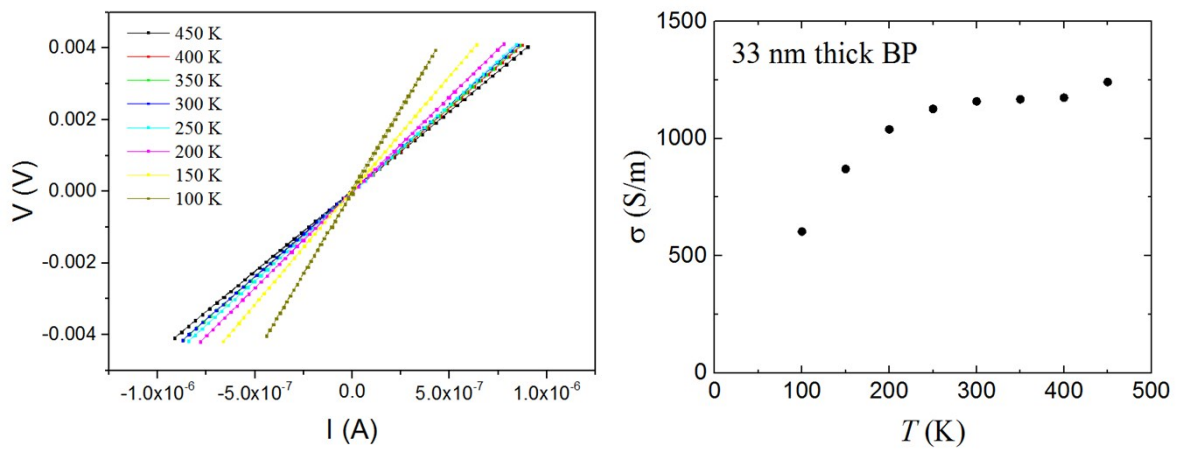


Figure S2. (a) I-V curves with temperature, which were measured for 33 nm-thick BP NS by a four-point probe method, and (b) Variation of electrical conductivity with temperature evaluated using the I-V curves.

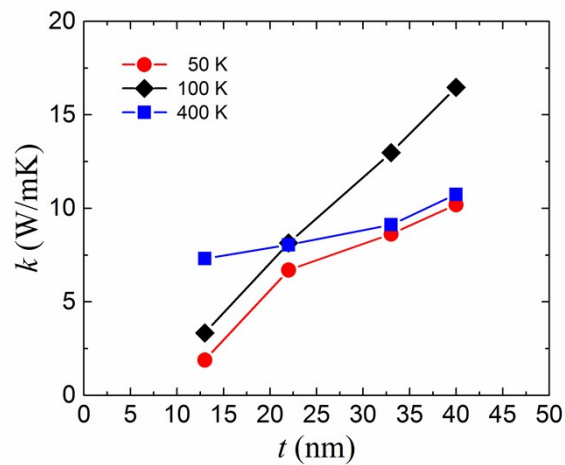


Figure S3. Variations of thermal conductivities with temperature and BP thickness.

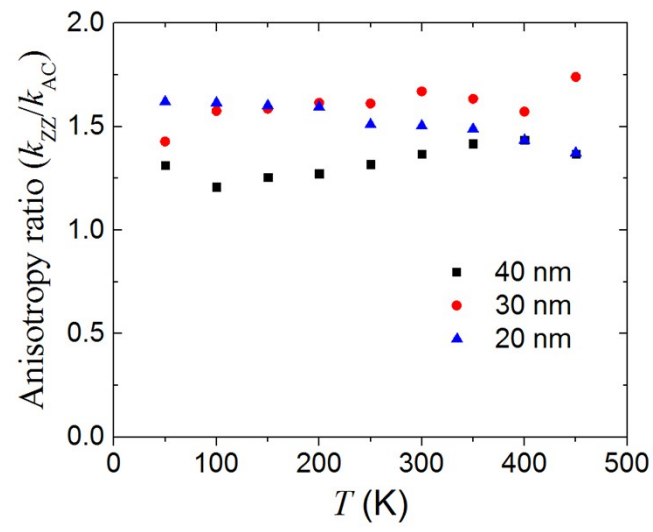


Figure S4. Variation of anisotropy ratio (k_{ZZ}/k_{AC}) with temperature and BP thickness.

Thermal conductivity measurement

The suspended structure of the microdevice was fabricated with 500 nm thick low-stress silicon nitride deposited on a silicon wafer using a lithography method. A Pt nanopattern including a nanoheater and a pair of thermometers were formed on the suspended silicon nitride. The back-side silicon beneath the suspended structure was etched away by an anisotropic wet etching process in a KOH solution.

The temperature coefficient of resistance (*TCR*) of the Pt thermometers were used in order to determine the temperature at two thermometers, which was done by converting the resistance change (ΔR) to the temperature change (ΔT) with the TCR values in the temperature range of 50 K to 450 K. The surrounding temperature in the chamber was read with a Si diode sensor (D-670 Lake Shore).

In thermal conductivity measurement, we adopted a heat conduction model based on the Fourier law, $Q = G\Delta T$, where Q , ΔT , and G are heat dissipation (W, J/s) by Joule heating, temperature difference (K) between the hot and cold sides, and thermal conductance (W/K) of the BP nanosheet (NS), respectively. The effects of heat radiation and residual gas convection were assumed to be negligible in this work.

The thermal conductivity of a BP NS can be determined by comparing two measurements, namely ‘with’ and ‘without’ a BP NS. We used the measurement for ‘without’ as a reference. In the microdevice without a BP NS, the heat dissipation (Q_1) in the steady state can be written as below,

$$Q_1 = G_1(T_{h,1} - T_o) \quad \text{Eq.(1)}$$

Here, Q_1 is equal to the heat energy generated by the joule heating at the nanoheater; G_1 is the thermal conductance of the microdevice through the silicon nitride structures; $T_{h,1}$ and T_o are the temperatures at the hot side and environment (heat-sink), respectively. In the case

of the microdevice with a BP NS, the heat is dissipated through both the Si nitride structures and the BP NS. Therefore, the heat transfer in the microdevice can be described as below,

$$Q_2 = Q'_1 + Q_{NS} \quad \text{or}$$

$$Q_2 = G_1(T_{h,2} - T_o) + G_{NS}(T_{h,2} - T_{c,2}) \quad \text{Eq.(2)}$$

Here, Q'_1 and Q_{NS} are the heat dissipation through the Si nitride structures and the BP NS. G_{NS} is the thermal conductance of the NS, and $T_{h,2}$ and $T_{c,2}$ are the temperatures at the hot and cold sides, respectively. As a result, the thermal conductance of a BP NS is expressed as

$$G_{NS} = \{Q_2 - G_1(T_{h,2} - T_o)\} / (T_{h,2} - T_{c,2}) \quad \text{Eq.(3)}$$

It was assumed that the thermal conductance (G_1 and G_{NS}) remains constant within a small temperature change (<10 K). The thermal conductivity of the BP NS (k_{NS}) is calculated according to the following Eq.(4),

$$k_{NS} = G_{NS}(L/A) \quad \text{Eq.(4)}$$

Here, A is the cross-sectional area and L is the length of the NS.

Measurement uncertainty analysis

As the thermal conductivity is defined as $k = G(A/L)$, (G , A and L are thermal conductance, cross-section area, and length of the NS), a combined uncertainty model can be written according to the law of uncertainty propagation as Eq.(5)

$$\left(\frac{u(k_{NS})}{k_{NS}}\right)^2 = \left(\frac{u(G_{NS})}{G_{NS}}\right)^2 + \left(\frac{u(A_{NS})}{A_{NS}}\right)^2 + \left(\frac{u(L_{NS})}{L_{NS}}\right)^2 \quad \text{Eq.(5)}$$

The $u(k_{NS})$ is a combined uncertainty composed of three standard uncertainties of $u(G_{NS})$, $u(A_{NS})$, $u(L_{NS})$. And the thermal conductance of a BP NS is given, following Eq.(3), as below

$$G_{NS} = \frac{Q - G_1(T_h - T_0)}{T_h - T_c} \quad \text{Eq.(6)}$$

Here, Q is the heat dissipation by Joule heating of the nanoheater; G_1 is the thermal conductance of the microdevice; T_h , T_c and T_0 are the temperature at the hot side, cold side, and the surrounding, respectively. Thus, the uncertainty terms of $u(Q)$, $u(\Delta T_h - \Delta T_c)$, $u(G_1)$, and $u(\Delta T_h - \Delta T_o)$ are needed to calculate the $u(G_{NS})$. By combining each uncertainty component, we express $u(G_{NS})$ as follow.

$$u(G_{NS}) = \sqrt{\left(\frac{u(Q)}{Q}\right)^2 + \left(\frac{u(G_1)}{G_1}\right)^2 + \left(\frac{u(T_h - T_0)}{T_h - T_0}\right)^2 + \left(\frac{u(T_h - T_c)}{T_h - T_c}\right)^2} \quad \text{Eq.(7)}$$

Considering the vendor specifications for the electronics used in this work (Keithley 2182A, Keithely 6221, and Signal recovery 5210), we determined at most

$\frac{u(R_i)}{R_i} = \sqrt{\left(\frac{u(V)}{V}\right)^2 + \left(\frac{u(I)}{I}\right)^2} \approx 2\%$ (i =heater, hot, and cold). Here R and I are resistance and current, respectively. Since the $u(I)/I$ is given to be $\sim 0.05\%$, we determined the relative

$$\text{uncertainty of } \frac{u(Q)}{Q} = \sqrt{\left\{2\frac{u(I)}{I}\right\}^2 + \left\{\frac{u(R)}{R}\right\}^2} \approx 2\%.$$

The uncertainty of the G_1 is determined with $u(Q)$ and $u(T_h - T_0)$ (Eq.(1)). The T_h is a temperature at the hot side, which is determined using the TCR ($\equiv dR/dT_o \sim \Delta R/\Delta T_o$) (slope or an estimated regression equation) of the Pt thermometer. In this case, T_h is known to have an

$$\text{uncertainty of } \sqrt{MSE \left[1 + \frac{1}{n} + \frac{(x_o - \bar{x})^2}{S_{xx}} \right]}, \text{ where MSE is Mean Square Error, } S_{xx} = \sum_{i=1}^n (x_i - \bar{x})^2,$$

and \bar{x} is an average value. Figure S5 shows an R vs. T curve used for the TCR calibration at 350 K. When T_h is 350 K, the relative uncertainty is calculated to be about 0.02 %. In addition, the R and T measurements also contain their own uncertainties, $u(R)$ and $u(\Delta T_o)$ (T_o is the temperature given by a Si diode sensor). According to the vendor specification, the T_o has an uncertainty of 32 mK at 300 K (Lake Shore DT-670). Taking into account the temperature fluctuation of the cryostat of ~ 50 mK, we determined the uncertainty for the T_o as $u(T_o) = \sqrt{0.032^2 + 0.050^2}$ mK = 59 mK. When $T_o = 350$ K, the relative uncertainty

$$\text{of } T_o \text{ should be estimated to be } \frac{u(T_o)}{T_o} = \frac{59 \text{ mK}}{350 \text{ K}} \approx 0.02\%.$$

$$T_h \text{ is expressed as } \frac{u(T_h)}{T_h} = \sqrt{0.0002^2 + 0.0002^2 + 0.02^2} \approx 2\%.$$

$$\frac{u(T_h - T_0)}{T_h - T_0} = \sqrt{0.02^2 + 0.0002^2} \approx 2\%. \quad \text{Consequently, } \frac{u(G_1)}{G_1} = \sqrt{0.02^2 + 0.02^2} = 2.8\%$$

Since Pt thermometers at the hot and cold sides have the same dimensions, it is reasonably

assumed, $u(T_h) = u(T_c)$. Therefore, we obtained $\frac{u(T_h - T_c)}{T_h - T_c} = \sqrt{2} \cdot 2\% = 2.8\%$. We note that the thermal conductance of the BP NS is determined by the difference in G . In practice, we can find the G_{NS} by subtracting the G for ‘with NS’ from ‘without NS’. Then, the

uncertainty of G_{NS} is written as $u(G_{NS}) = u^2\left(\frac{Q}{T_h - T_c}\right) + u^2\left(\frac{G_1(T_h - T_0)}{\Delta T_h - \Delta T_c}\right)$ or

$$\frac{u(G_{NS})}{G_{NS}} = \sqrt{\left[u\left(\frac{Q}{T_h - T_c}\right) / \left(\frac{Q}{T_h - T_c}\right)\right]^2 + \left[u\left(\frac{G_1(T_h - T_0)}{\Delta T_h - \Delta T_c}\right) / \left(\frac{G_1(T_h - T_0)}{\Delta T_h - \Delta T_c}\right)\right]^2} = 5.6\%.$$

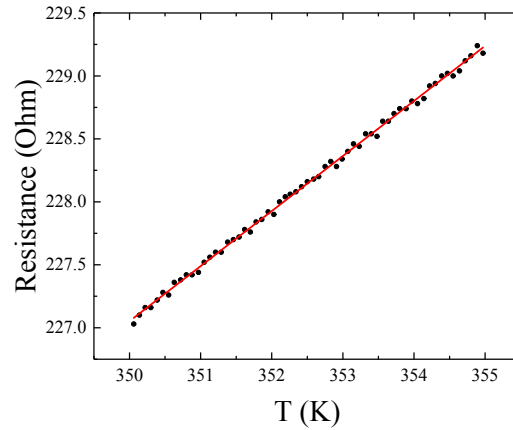


Figure S5. R vs. T curve for TCR calibration.

When it comes to the measurement uncertainty of k_{NS} in Eq.(5), the $u(A_{NS})$ and $u(L_{NS})$ are also needed to be evaluated. We measured the length of the BP NS using a SEM, which has a spatial resolution less than 2 nm. For a 3 μm long BP NS, we calculated $u(L)/L$ much less than 0.1%. In thickness measurement, we used an atomic force microscope in tapping mode. The uncertainty of AFM measurement is estimated to be $\approx 2\%$ for 13 nm BP NS ($u(t)/t = 0.3 \text{ nm}/13 \text{ nm} \approx 2\%$). Finally, we have verified that

$$\frac{u(k_{NS})}{k_{NS}} = \sqrt{\left(\frac{u(G_{NS})}{G_{NS}}\right)^2 + \left(\frac{u(A_{NS})}{A_{NS}}\right)^2 + \left(\frac{u(L_{NS})}{L_{NS}}\right)^2} = 5.9 \%$$
 This uncertainty is expanded to be 13.6 % with a $t_{(n-2, \alpha/2)}$ value of 2.31 at 95 % confidence level for $n > 10$. Including the random effects occurring in measurement processes, we showed the total uncertainty with error bars in figure 2. In addition to that, an angular deviation of the BP NS would be another source of uncertainty. A 10 degree deviation could leads to about 4 % change in thermal conductivity [S1].

Table S1. Relative uncertainty components in percentage terms [%]

$u(Q)/Q$		2.0	$u(T_h - T_c)$		2.8
$u(R)/R$	2.0		$u(T_h)$	2.0	
$u(I)/I$	0.050		$u(T_c)$	2.0	
$u(G_1)/G_1$		2.8	$u(T_h - T_0)$		2.0
$u(Q)/Q$	2.0		$u(T_h)$	2.0	
$u(T_h - T_0)/(T_h - T_0)$	2.0		$u(T_0)$	0.020	
$u(A)/A$		0.10	$u(L)/L$		2.0

Regarding the thermal contact resistance (R_c), we roughly estimated the thermal contact resistance based on the rectangular fin model [S2, S3] as below,

$$R_c = \frac{1}{4} \frac{1}{\sqrt{hPkA_c} \tanh \sqrt{\frac{hP}{kA_c} L_c}}$$
 , where h , L_1 , P , k , A_c , and L_c are the heat transfer coefficient, interface thickness, contact width, thermal conductivity, cross-sectional area, and contact overlap length. For convenience, h was assumed to be k_l/L_1 , K_l interface thermal conductivity and L_1 interface length, respectively [S3]. The R_c is calculated to be ~ 0.15 K/ μ W as the

maximum value for the thinnest BP NS (13 nm thick, 10 μm wide), when $P=5 \mu\text{m}$, $k=5 \text{ W/mK}$, and $A_c=1.3\times 10^{-13} \text{ m}^2$ are used. Given the thermal resistance of 2.01 K/ μW for the thinnest BP NS (13 nm thick, 10 μm wide), the calculated R_c of 0.15 K/ μW is approximately 8 % of our measurement. However, we deposited Pt on the thermal contacts using FIB in order to increase the contact areas as well as to eliminate air gaps between the BP NS and the Pt thermometer. Therefore, the contact resistance would be negligible in our case.

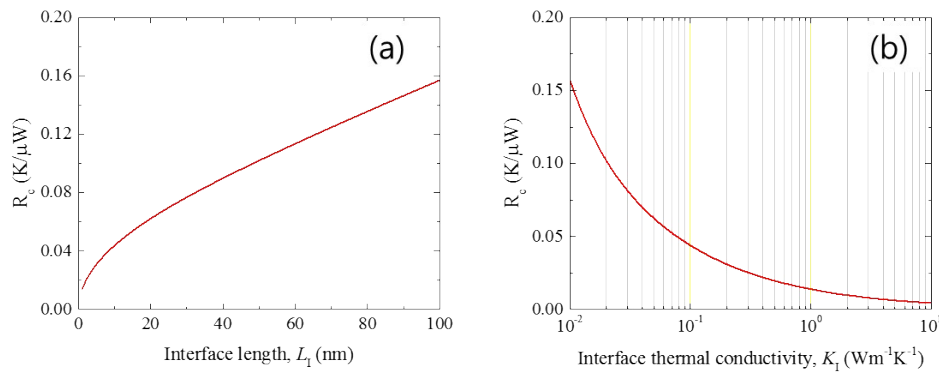


Figure S6. Calculated thermal contact resistance (R_c) with (a) interface length L_1 and (b) interface thermal conductivity K_1 .

Notes and references

1. Liu T and Chang C 2015 *Nanoscale* **7** 10648
2. Incropera F P, Dewitt D P, Bergman T L and Lavine A S 2014 *Principles of Heat and Mass Transfer 7th ed.* Willey
3. Jia Z, Hippalgaonkar K, Shen S, Wang K, Abate Y, Lee S, Wu J, Yin X, Majumdar A and Zhang X 2014 *Nano Lett.* **14** 4867